Emissive chart for imager calibration

Jeffrey M. DiCarlo, Glen Eric Montgomery and Steven W. Trovinger
Hewlett-Packard Laboratories
Palo Alto, California

Abstract

Each and every color imaging device should be custom calibrated both to enhance image processing algorithms and to produce pleasing and faithful images of the captured scenes or medias. Custom calibrations, however, are usually not performed because calibration instruments are either too slow to be used on the manufacturing line or the instruments lack the necessary accuracy. We have developed a calibration instrument that enables both fast and accurate imager calibrations. The instrument is based on emissive narrow-band light sources—light emitting diodes—arranged in a grid pattern or chart configuration. We refer to the instrument as the *emissive calibration chart* or the *EC chart*. We compare the emissive calibration chart to other calibration instruments, which include reflective charts, like the Macbeth ColorChecker or DC charts, and monochromators. The results demonstrate that custom calibrations of each and every imager could be accurately determined on the manufacturing line using the emissive calibration chart.

1. Introduction

Color imaging systems, *e.g.,* cameras, scanners, copiers, etc., should be calibrated both to (a) increase the accuracy of various image processing algorithms used in the devices [1], which includes color correction [2,3] and illuminant estimation [4,5] algorithms, and to (b) produce pleasing and faithful color images and reproductions of the captured scenes or medias [6]. Calibration involves the measurement of the imaging system's responsivity functions as well as its transduction function. These functions determine how any imager responds to incident light signals [7,8].

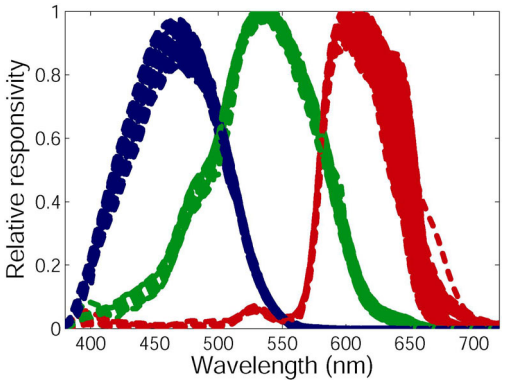

Figure 1. *Responsivity functions for two hundred instances of a consumer camera plotted on top of one another. The widths of the lines indicate the responsivity variations across camera instances.*

Typically, the calibration information required for an imaging system is measured once for a particular device model, and the information is assumed constant across all instances of the devices. This assumption, however, is usually incorrect. Figure 1 illustrates the large variations between the responsivity functions of different instances of a consumer camera. Two hundred camera responsivity functions are plotted on top of one another. The widths of the lines indicate the expected variation in the responsivity functions. By failing to calibrate for these variations in each device, a camera may produce objectionable color reproductions, which may lead to customer dissatisfaction.

Although it is generally recognized that the custom calibration of each and every imaging device is desirable, it has not been achieved due to inadequate calibration instruments. Current calibration instruments are either too slow to be used on the manufacturing line or the instruments do not produce the required accuracy.

In this paper, we introduce a new calibration instrument that enables both fast and accurate imager calibrations. Section 2 explores the background mathematics behind imager calibration and outlines the theory that defines an accurate calibration instrument. Section 3 describes current calibration instruments and highlights their main advantages and disadvantages. Section 4 presents an *emissive calibration chart* or *EC chart* that either equals or exceeds current calibration instruments in terms of speed and accuracy. Finally, Section 5 compares the calibrations obtained with the EC chart and conventional calibration instruments.

2. Calibration Theory

Calibration of an imaging device is the estimation of the imaging system's responsivity and transduction functions. These functions determine how any imager responds to incident light signals [9]. In this section, we explore the background mathematics behind imager calibration and outline the general theory that defines whether a calibration instrument can produce accurate estimates of an imager's responsivity functions. We focus on an imager's responsivity functions because CCD and CMOS

transduction functions tend to be highly linear and, therefore, straightforward to estimate.

An imager's responsivity functions are used to map the spectral power distributions of incident light signals to an imaging device's sensor responses. This mapping, known as the image formation equation, is defined in Equation 1. In the equation, **L** is matrix where the j^{th} column contains the spectral power distribution of the j^{th} incident light signal, **R** is a matrix where the i^{th} column contains the responsivity function the i^{th} image sensor, and **S** is a matrix where the $s_{i,j}$ element is the response of the i^{th} image sensor due to the j^{th} incident light signal.

$$\mathbf{S} = \mathbf{R}^{\mathrm{T}}\mathbf{L} \qquad (1)$$

Calibration of an imager is the computation of the imager responsivity functions (**R**) from the imager responses (**S**) that arise from capturing of a small set of known incident light signals (**L**). In other words, it is the inversion of Equation 1 to solve for **R** when **L** is known and **S** is measured. The quality or accuracy of the solution, however, depends directly on the spectral power distributions of the incident light signals generated by a calibration instrument. Specifically, it depends on the singular values of an instrument's incident light signals. The more normalized singular values of **L** greater than a fixed constant, the better the estimated responsivity functions produced by a calibration instrument.

The **L** matrix generated by any calibration instrument can be written in terms of its singular value decomposition, $\mathbf{L} = \mathbf{U}\mathbf{D}\mathbf{V}^{\mathrm{T}}$ [10]. Here, **U** and **V** are orthonormal matrices and **D** is a diagonal matrix, where the diagonal elements of **D** are all positive and monotonically decrease from the upper-left element to the lower-right element. The diagonal elements of **D** are known as the singular values of **L**. These singular values when normalized by the first singular value, *i.e.*, $[d_{1,1}/d_{1,1}, d_{2,2}/d_{1,1}, \ldots, d_{N,N}/d_{1,1}]$, indicate the accuracy of the responsivity estimates obtainable using a particular calibration instrument.

We illustrate the dependence of the responsivity estimates on the singular values of **L** by inverting the image formation equation. There are many inversion techniques to estimate an imager's responsivity functions [10, 11, 12, 13, 14]. Here, we use a common technique, the pseudo-inverse, to simplify the derivation, but similar results can be shown using any other technique. Equation 2 shows the estimated responsivity functions using the pseudo-inverse and the singular value decomposition of **L**. In the equation, $\hat{\mathbf{R}}$ is a matrix containing the estimated responsivity functions as columns; **S** are the imager responses to the **L** matrix; **U**, **D**, and **V** represent the singular value decomposition of **L**; and α is a user-defined tolerance constant.

$$\hat{\mathbf{R}} = \mathbf{U}\mathbf{D}^{+}\mathbf{V}^{\mathrm{T}}\mathbf{S}^{\mathrm{T}}, \text{ where } \mathbf{D}^{+} = \begin{cases} 1/d_{i,i} & \text{for } d_{i,i}/d_{1,1} > \alpha \\ 0 & \text{otherwise} \end{cases} \qquad (2)$$

Equation 2 illustrates the effect of the singular values of **L** (elements of **D**) on the estimated responsivity functions. Specifically, it shows that the estimated responsivity functions are a linear function of the measured imager responses, and more importantly, the number of degrees of freedom contained in the linear function is equal to the number of normalized singular values of **L** that are greater than α. Singular values that are less than α are set to zero and not inverted. When a singular value is set to zero, it reduces the degrees of freedom in the final estimates, but as we describe later in this section, it also constrains any sensor noise from affecting the estimated responsivity functions.

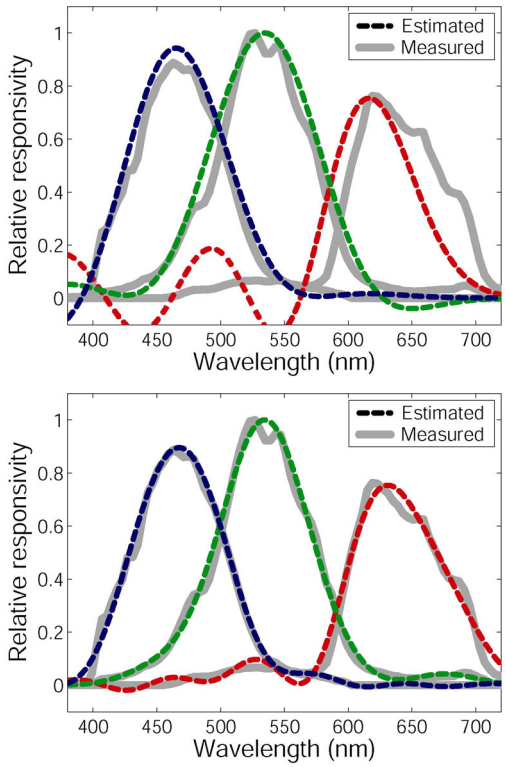

Figure 2. *The responsivity functions estimates of a camera obtained using two simulated calibration instruments: (top) Instrument 1, (bottom) Instrument 2. Instrument 2 contains more normalized* ***L*** *singular values greater than α. See text for details.*

Figure 2 shows an example of the responsivity estimates of a camera obtained using two simulated calibration instruments. We refer to them as Instrument 1 and 2. The color-dotted curves are the responsivity estimates and the gray-solid curves are the measured responsivity functions. The top panel shows responsivity estimates obtained from Instrument 1, and the bottom panel shows the responsivity estimates obtained from Instrument 2. The normalized **L** singular values of Instrument 1 are [1, 0.75, 0.46, 0.24, 0.11, 0.041, 0.013, 0.003, …], and the values of Instrument 2 are [1, 0.94, 0.84, 0.73, 0.61, 0.49, 0.37, 0.28, 0.19, 0.13, 0.08, …]. Both panels use a tolerance of α = 0.1.

Figure 2 shows that the estimated responsivity functions in the bottom panel track the measured responsivity functions much better than the responsivity estimates in the top panel. Instrument 2, the bottom panel, has ten **L** singular values greater than α; thus, it produces estimates with ten degrees of freedom. Instrument 1, the top panel,

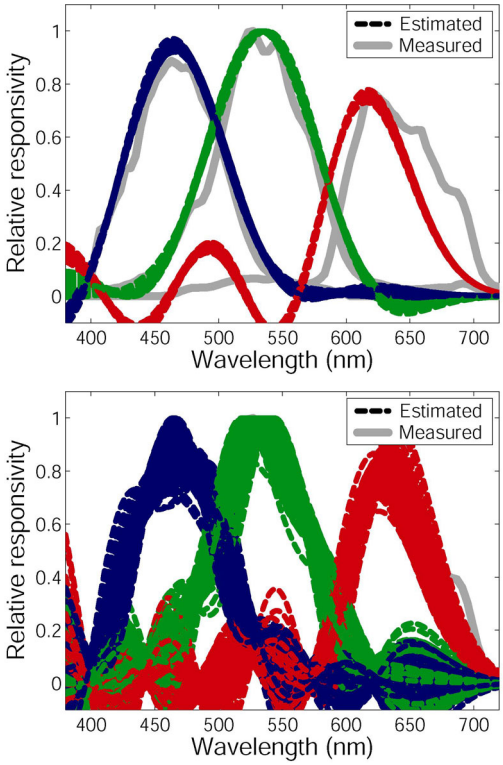

Figure 3. *The variance of the estimated responsivity functions for Instrument 1 using two different α values: (top) one hundred responsivity estimates for α = 0.1 and, (bottom) one hundred responsivity estimates for α = 0.01*

has five **L** singular values greater than α: it produces estimates with five degrees of freedom. Because Instrument 2 produces more degrees of freedom for a fixed α, its estimates track variations in the measured responsivity functions much better than Instrument 1.

It may appear from Equation 2 and Figure 2 that accurate responsivity estimates can be generated from Instrument 1 if α is set closer to zero. After all, an α value close to zero would enable more singular values of **L** to be inverted and would maximize the number of degrees of freedom in the final estimates. There is, of course, a down-side to including small singular values in the pseudo-inverse: the estimation variance grows inversely with the singular values *squared.*

Equation 3 shows the variance of the responsivity estimates using the pseudo-inverse. In the equation, $\mathbf{\Sigma}_{\hat{\mathbf{R}}}$ is the variance of the estimated responsivity functions; $\mathbf{\Sigma}_{\mathbf{S}}$ is the variance of the measured imager responses; σ_S^2 is an approximation of $\mathbf{\Sigma}_{\mathbf{S}}$, assuming a constant imager response variance; and **U**, **D**, and **V** are the singular value decomposition matrices of **L**.

$$\begin{aligned}\mathbf{\Sigma}_{\hat{\mathbf{R}}} &= \mathbf{U}\mathbf{D}^{+}\mathbf{V}^{T}\mathbf{\Sigma}_{\mathbf{S}}\mathbf{V}\mathbf{D}^{+}\mathbf{U}^{T} \\ &\approx \mathbf{U}\mathbf{D}^{+}\mathbf{D}^{+}\mathbf{U}\sigma_S^2\end{aligned} \qquad (3)$$

Equation 3 illustrates that the estimated responsivity function variance is inversely proportional to the square of the **L** singular values greater than α. Setting a small value of α, while it increases the number of degrees of freedom, amplifies any noise in the measured imager responses.

Figure 3 illustrates the effect of decreasing α for Instrument 1 shown in the top panel of Figure 2. Each panel contains one hundred responsivity functions that were estimated by including noise in the simulated responses. The noise distribution assumed was Gaussian with mean zero and a standard deviation of 1 bit for an 8 bit imager. The top panel shows estimates for α = 0.1, and the bottom panel shows estimates for α = 0.01. We can see from the bottom panel that lowering α to 0.01 greatly increases the sensitivity of the responsivity estimates to noise in the imager responses, producing unreliable estimates.

In this paper, we compare calibration instruments by examining the normalized singular values of the incident light signals generated by each instrument. Specifically, we compare the instruments by counting the number of singular values that are greater than a fixed value of α. The comparison equalizes the estimated variance of the different calibration instruments. The more singular values an instrument has above α, the better is ability to track variations in the responsivities; hence, the more accurate the estimates and the better the calibration instrument.

3. Calibration Instruments

Currently, most calibration instruments can be categorized as either (a) reflective charts or (b) monochromators. Both instruments are used for calibrating imagers, but as we discuss in the following subsections, neither instrument is well-suited for calibrating imagers both quickly and accurately.

3.1. Reflective charts

Reflective charts are calibration instruments that usually consist of multiple color patches pasted onto a cardboard backing. Examples of reflective charts include the Macbeth ColorChecker [15] and the Macbeth DC chart. The Macbeth ColorChecker chart consists of twenty-four color patches and the Macbeth DC chart consists of over two-hundred color patches. These charts and reflective charts in general must be uniformly illuminated with a stable light source to calibrate a camera sensor.

The light reflected from the individual color patches defines the incident light signals used to calibrate an imager. Specifically, if we assume **P** is a matrix of surface reflectance functions, where each column represents the reflectance function of a patch in the reflective chart, and **e** is the spectral power distribution of the stable light source, then the incident light signal matrix, **L**, is defined as **L** = diag(**e**)**P**, where diag(**x**) represents placing the vector **x** in a diagonal matrix.

The main advantage of reflective charts as calibration instruments is the spatial layout of the color patches in a grid format. The layout allows for multiple incident light signals to be simultaneously captured by an imaging device. Only one capture is usually required; thus, the time necessary to

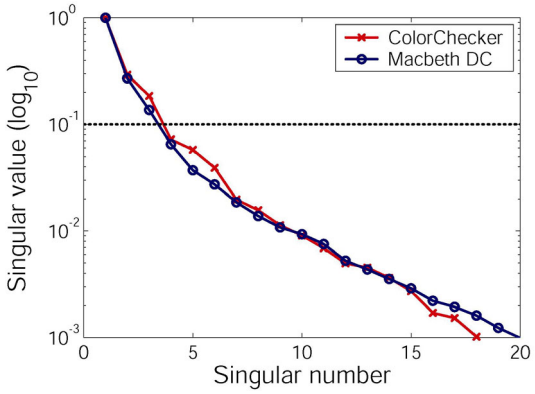

Figure 4. *Singular values of the incident light signals from two reflective charts: the Macbeth ColorChecker and DC chart.*

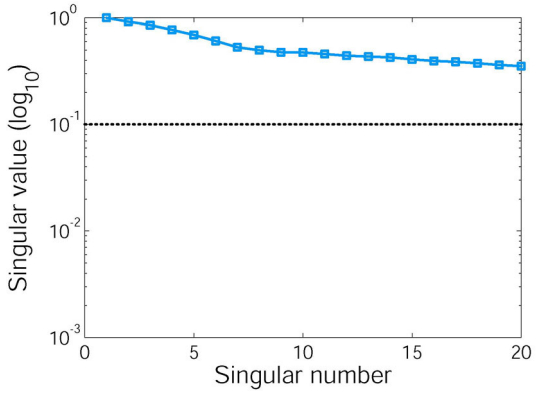

Figure 5. *Singular values of the incident light signals from a typical monochromator.*

complete a calibration is very short. This, however, is one of the only advantages of reflective charts. Reflective charts we have tested to date produce inaccurate calibration results. The **L** singular values of reflective charts decrease too rapidly due to correlation between patch colors.

Figure 4 shows the singular values of the incident light matrix for the ColorChecker and the DC charts. In both cases, a fluorescent light source was used to uniformly illuminate the charts. As evident from the figure, the singular values of the charts decrease rapidly. The black dotted line indicates the pseudo-inverse tolerance value (α = 0.1) required to limit the standard deviation of the estimated responsivity functions to +/– 4% for an 8 bit imager. At this setting, the estimated responsivity functions have only three degrees of freedom. Three degrees is too few to track variations in common imager responsivity functions (See Section 5).

3.2. Monochromators

The other category of calibration instruments are monochromators. Monochromators are devices that can filter a broad-band light source into a narrow-band light source centered at a specified wavelength. The Oriel MS257 is an example of a monochromator.

On the input side of a monochromator is a broad-band light source. The broad-band light is fed through a complex optical system that consists of lenses, slits and diffraction gratings. At the output of the monochromator, illumination with a spectral power distribution that is narrow-band and centered at a specified wavelength is generated. Typically, the narrow-band illumination is fed into an integrating sphere to produce a spatially uniform output. It is this uniform, narrow-band illumination that defines one column of the incident light signal matrix, **L**, for monochromators. Another incident light source (column of **L**) is produced by electronically controlling the monochromator to produce a narrow-band signal centered at a different wavelength. Sweeping the monochromator through many different center wavelengths generates all the incident light signals.

Monochromators are advantageous as calibration instruments because they produce accurate responsivity estimates. Each narrow-band light output at one wavelength is usually independent of the narrow-band light output at another wavelength. Independence between incident light signals translates to **L** singular values that decrease slowly.

Figure 5 shows the singular values for a monochromator. As in Figure 4, the black dotted line indicates the pseudo-inverse tolerance value (α = 0.1) necessary to limit the standard deviation of the estimated responsivity functions to +/– 4% for an 8 bit imager. Monochromators have many singular values greater than α; thus, the responsivity estimates can track variations in the imager sensors. Unfortunately, monochromators generate incident light signals sequentially. An imager must capture multiple images for a complete calibration: one image for each light signal. Calibration can take upwards to an hour even if everything is automated. This greatly limits their use for calibrating imagers on the manufacturing line.

4. Emissive calibration chart

A hardware and software solution called the *emissive calibration chart* or *EC chart* enables both fast and accurate calibrations of an imager's responsivity and transduction functions. The hardware of the EC chart is based on emissive light sources configured to resemble a reflective chart. A photograph of the first prototype EC chart is shown in Figure 6. The chart consists of multiple light sources; an electronic control board for setting the intensities of the light sources; and optical components that randomize and diffuse the light to produce various colored uniform patches at the output of the device.

The EC chart innovation that enables both quick and accurate calibration of an imager is the use of multiple light sources that are both spatially and spectrally separated. The spatial separation of the light sources in a grid arrangement—similar to reflective charts—allows for quick calibrations. Only a single image is required to capture the imager's response to each light source. The use of spectrally separated narrow-band light sources—similar to the light output of a monochromator—enables accurate calibrations. The EC chart integrates the best features of reflective charts and monochromators into one calibration instrument.

Figure 6. *The first prototype of the emissive calibration chart.*

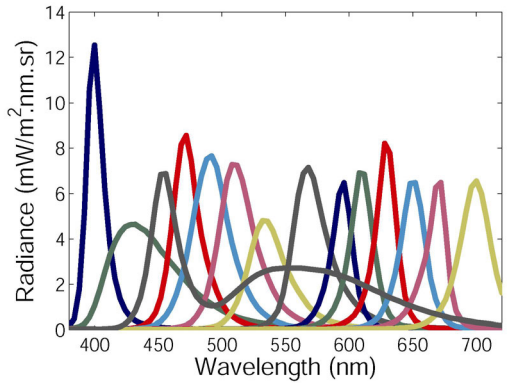

Figure 7. *The spectral power distributions of the LED light sources used in the emissive calibration chart.*

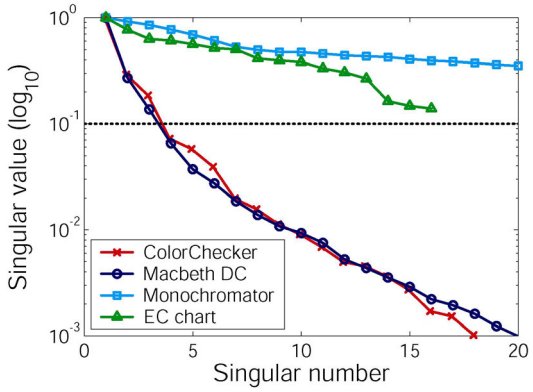

Figure 8. *Singular values of the incident light signals from the EC chart and other instruments.*

The calibration of an imager using the EC chart consists of two quick and simple steps: (a) capture an image of the EC chart, and (b) run software to determine the imager's responsivity functions. The software extracts the patches from the captured image and with knowledge of the spectral power distribution of the light sources, inverts the image formation equation to estimate the imager responsivity functions. The entire calibration time is comparable to that of reflective charts and is orders of magnitudes faster than monochromators. A camera can easily be calibrated in less than thirty seconds.

Figure 7 illustrates the spectral power distributions of the light sources that we used in the first EC chart prototype. The light sources used were light-emitting diodes (LEDs) at various wavelengths. A total of sixteen different LEDs were used (two are not shown). The spectral power distributions of these sources define the incident light signals matrix, **L**.

Figure 8 shows the singular values of the incident light matrix compared with those of reflective charts and monochromators. These singular values determine the variance of the estimated responsivity functions of an imager using the EC chart (See Section 2). As in Figures 4 and 5, the black dotted line indicates the pseudo-inverse tolerance value ($\alpha = 0.1$) required to limit the standard deviation of the estimated responsivity functions to +/– 4%. We can see that all sixteen light sources can be used in the calibration; hence, any estimated responsivity functions have sixteen degrees of freedom. Sixteen degrees of freedom enable the estimates to accurately track the responsivity functions of typical imagers.

5. Results

Figure 9 compares the calibration performance of the EC chart against two reflective charts, the Macbeth ColorChecker and the Macbeth DC, and an Oriel MS257 monochromator. Specifically, it shows the estimated responsivity functions for a Nikon D1 digital camera. The top panel illustrates the estimated responsivity functions using the Macbeth ColorChecker, the middle panel illustrates the functions using the Macbeth DC chart and the bottom panel illustrates the functions using the EC chart. In all the panels, the colored-dashed lines are the estimated responsivity functions and the solid-gray lines are the measured responsivity functions. The measured responsivities were computed using the monochromator, the most accurate calibration instrument.

All the responsivity functions were estimated using an inversion method similar to the pseudo-inverse discussed in Section 2 except the method constrained the responsivity estimates. Specifically, the method constrained the estimates to be all positive and used a smoothing interpolator to produce continuous first-derivative functions (See [13] for more details). The same tolerance value ($\alpha = 0.1$) was used for all estimates to equalize the estimation variance. As evident from the plots, the Macbeth ColorChecker and DC chart estimates were not able to track the variations in the measured responsivity functions due to a limited number of degrees of freedom at the specified tolerance value, while the EC chart was able to track the measured responsivity variations. The EC chart produced a more accurate camera calibration than both reflective charts. Furthermore, its calibration results were comparable to those of a monochromator, but were produced in less than 1% of the time.

As in Section 2, it can be argued that estimates produced by reflective charts in Figure 9 are not accurate because the tolerance value α was set too high. Figure 10 illustrates the effects of lowering α to 0.01 for the Macbeth ColorChecker. The top panel shows the estimated responsivity functions for a single calibration of the Nikon

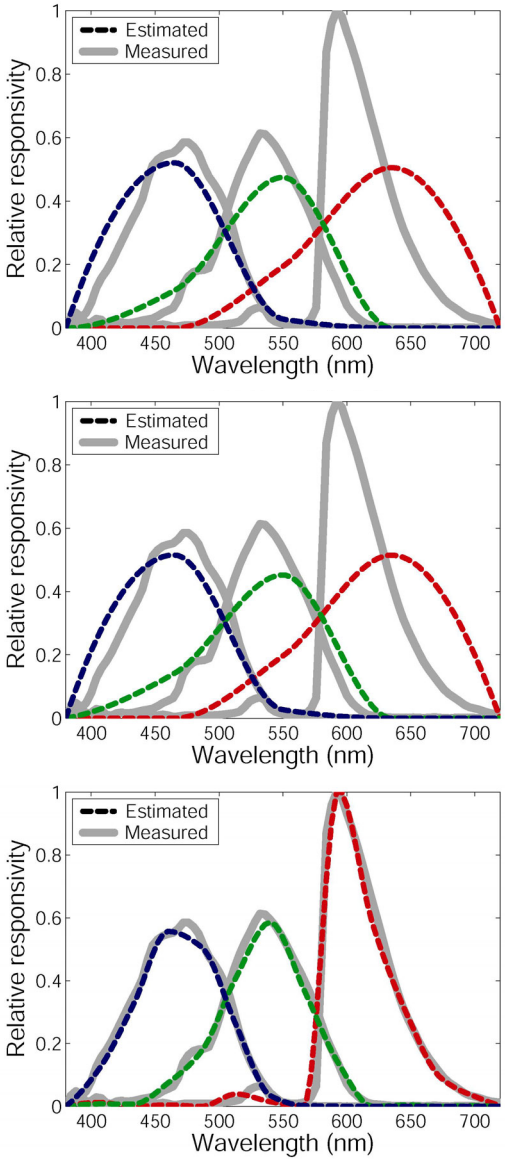

Figure 9. *Calibration results of a Nikon D1 camera using (top) the Macbeth ColorChecker, (middle) the Macbeth DC chart, and (bottom) the emissive calibration chart. The measured responsivities were made using an Oriel MS257 monochromator.*

D1 camera. As expected, the reduction in α enables the responsivity estimates to track the measured responsivity functions better because the estimates have more degrees of freedom. The bottom panel, however, illustrates the unreliability of the estimates with α = 0.01. The panel shows fifty calibrations of the same Nikon D1 camera using the same Macbeth ColorChecker. The noise variations in the camera responses cause the responsivity estimates to vary too widely for accurate camera calibrations.

6. Conclusion

We have tested the emissive calibration chart versus conventional calibration instruments, which included two

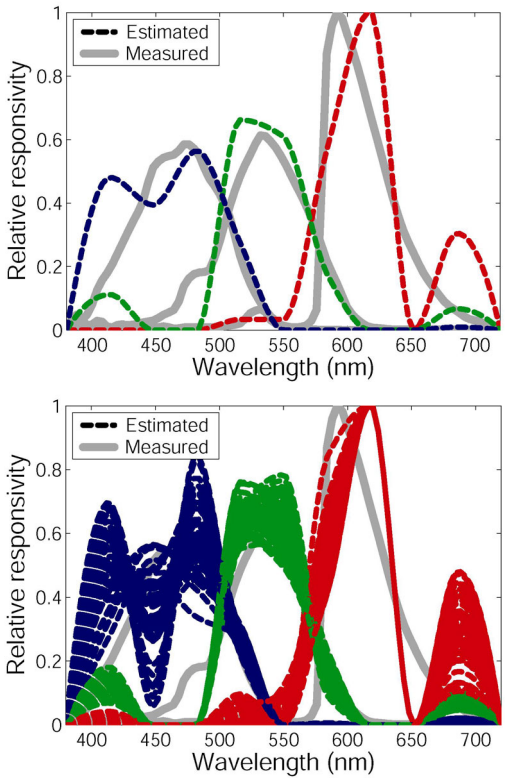

Figure 10. *The effects of calibrating a Nikon D1 camera using the Macbeth ColorChecker and α = 0.01: (top) the estimated responsivity functions from a single calibration and, (bottom) the estimated responsivity functions from fifty calibrations of the same Nikon D1 camera using the same Macbeth ColorChecker.*

reflective charts and a monochromator. The emissive calibration chart has numerous advantages over these instruments. Specifically, the chart has comparable accuracy to a monochromator, but it produces calibrations in less than 1% of the time required for monochromator calibration. For reflective charts, like the Macbeth ColorChecker or DC chart, the emissive calibration chart has comparable calibration speed, but it produces estimates with approximately thirteen more degrees of freedom, leading to more accurate imager calibrations. We believe the emissive calibration chart is the first calibration instrument that is quick enough to calibrate imagers on the manufacturing line and accurate enough to produce useful calibration results.

References

[1] J. Adams, K. Parulski and K. Spaulding, *Color processing in digital cameras*, IEEE Micro **18** (1998), no. 6, 20-29.

[2] G. Sharma, "Target-less scanner color calibration," *The seventh color imaging conference: Color science, systems and applications*, The society for imaging science and technology, Springfield, VA, 1999, pp. 69-74.

[3] J. M. DiCarlo, N. Sampat, M. Bhachech, M. McGuire and G. Dispoto, "Building a fine art reproduction system from

standard hardware," *Spie electronic imaging conference*, vol. 5017B, San Jose, CA, 2004.

[4] G. D. Finlayson, P. M. Hubel and S. Hordley, "Color by correlation," *Proceedings of the fifth color imaging conference*, Springfield, VA, 1997, pp. 6-11.

[5] J. M. DiCarlo, F. Xiao and B. A. Wandell, "Illuminating illumination," *Proceedings of the ninth coloring imaging conference*, Springfield, VA, 2001, pp. 27-34.

[6] R. W. G. Hunt, *The reproduction of colour*, Tolworth, England, 1995.

[7] B. A. Wandell, *The synthesis and analysis of color images*, IEEE Transactions on Pattern Analysis and Machine Intelligence **9** (1987), 2-13.

[8] R. S. Berns, *Billmeyer and saltzman's principles of color technology*, (2000).

[9] G. Wyszecki and W. S. Stiles, *Color science: Concepts and methods, quantitative data and formulae*, (1982).

[10] G. Strang, *Introduction to linear algebra*, Wellesley-Cambridge Press, Wellesley, MA, 1998.

[11] K. V. Mardia, J. T. Kent and J. M. Bibby, *Multivariate analysis*, London, 1979.

[12] T. Kailath, A. H. Sayed and B. Hassibi, *Linear estimation*, 2000.

[13] T. Hastie, R. Tibshirani and J. Friedman, *The elements of statistical learning: Data mining, inference, and prediction*, (2001).

[14] R. A. Johnson and D. W. Wichern, *Applied multivariate statistical analysis*, Upper Saddle River, NJ, 2002.

[15] C. S. McCamy, H. Marcus and J. G. Davidson, *A color-rendition chart*, J. Applied Photographic **48** (1976), 777-784.